Incipient breaking of unsteady waves on sheared currents

Aifeng Yao and Chin H. Wu[a)]
Department of Civil and Environmental Engineering, University of Wisconsin-Madison, Madison, Wisconsin 53706

(Received 22 October 2004; accepted 22 June 2005; published online 29 July 2005)

Incipient breaking of unsteady waves on sheared currents is experimentally investigated. A new wave-generation technique, based on the iterative frequency-focusing concept with the consideration of effects of Doppler shift and current shear, is developed. The surface displacement, the wavelength, and the phase speed of waves at the breaking onset on shear currents are measured. It is found that the steepness of unsteady, incipient breaking waves is altered by the sign and magnitude of current shear (or vorticity). A current with a positive shear, as would be the case in a wind-driven current, reduces the steepness of an unsteady incipient breaking wave. A negatively sheared current, such as the jet-like ebb current at a tide inlet, leads to steeper incipient breaking waves. The magnitude of reduction/increase in wave steepness is proportional to the strength of a current shear. In particular, a negative shear can alter the wave steepness more significantly in comparison to a positive shear of the same magnitude. Interestingly, the trend of crest-trough asymmetry with respect to the change of a current shear is in contrast to the limiting wave steepness. A positively sheared current can dramatically increase crest-trough asymmetry for unsteady waves. Dimensionless amplitudes of unsteady waves at incipient breaking are well correlated with surface current drifts. Positive/negative surface drifts lead to the reduced/increased dimensionless wave amplitudes. However, the change in dimensionless wave amplitude of unsteady waves is much smaller than that of steady waves. © *2005 American Institute of Physics*. [DOI: 10.1063/1.2000276]

I. INTRODUCTION

Incipient breaking of unsteady waves on vertically sheared currents is of great interest to fundamental fluid dynamics research as well as maritime operations. Incipient breaking is defined as the highest wave just prior to breaking.[1,2] In the ocean, waves tend to be unsteady and often appear in wave groups.[3–5] In addition, waves rarely propagate without the presence of currents.[6,7] There are many situations where currents are sheared, established by wind forcing,[8] oceanic circulation,[9] jet-like ebb tide at river mouth,[10,11] proceeding breakers,[1] wake of moving objects,[2] stratification, or bottom topography change.[6] Evidence of coexistence of sheared currents and unsteady surface waves is therefore well recognized. In recent years, a good progress on quantifying contributions of waves and sheared currents to momentum, energy, and mass exchanges across the air-sea interface has been made.[12–14] However, a fundamental question on how sheared currents affect the onset of unsteady wave breaking remains open for further research.[15]

The role of surface current shear in incipient breaking waves has been addressed from the pioneering study by Banner and Phillips.[16] They showed that a thin wind-induced drift layer (i.e., a positive shear or a negative vorticity) can reduce the maximum height of a steady monochromatic wave at incipient breaking. Several theoretical studies[17–21] have further showed that appreciable variations in the steepness and crest shape of limiting can exist, depending on the magnitude and sign of shear. Detailed laboratory measurements and numerical simulations by Miller, Nennstiel, Duncan, Dimas, and Prostler[2] confirmed that the presence of a surface drift layer with positive shear reduces the maximum steady wave height. For the onset of unsteady wave breaking, the numerical studies by Banner and Tian[22] and Banner and Song[23] revealed a tendency of positive shear (wind drifts) in reducing the limiting steepness. In spite of the progress, there remains an acute shortage of measurements to further reveal unsteady incipient breaking waves traveling in vertically sheared currents.

Difficulty in realizing experiments on unsteady incipient breaking waves in the presence of sheared currents has been the main reason that impedes the progress of supportive measurements. The experimental challenge involves simultaneously generating unsteady waves on a sheared current. To create an unsteady wave breaking in the absence of a current, a dispersive focusing method has been successfully employed in laboratory facilities.[1,24,25] The concept is to arrange the initial phase shift of each frequency component in a wave packet so that an unsteady, isolated, extreme, or breaking wave can be formed. Recently, this method has been extended to unsteady waves on a depth-uniform current.[26] Despite the success, a downshifting of the actual focusing position has been identified.[1,27–29] This downshifting issue that causes the occurrence of unsteady incipient breaking waves not at the location with the designed current can be a concern for realizing well-controlled experiments.

In this paper, the downshifting of the actual focusing position is overcome by an iterative (nonautomated feedback control) frequency-focusing wave-generation method. In the following, the experimental approach including wave-current

a)Author to whom correspondence should be addressed. Electronic mail: chinwu@engr.wisc.edu

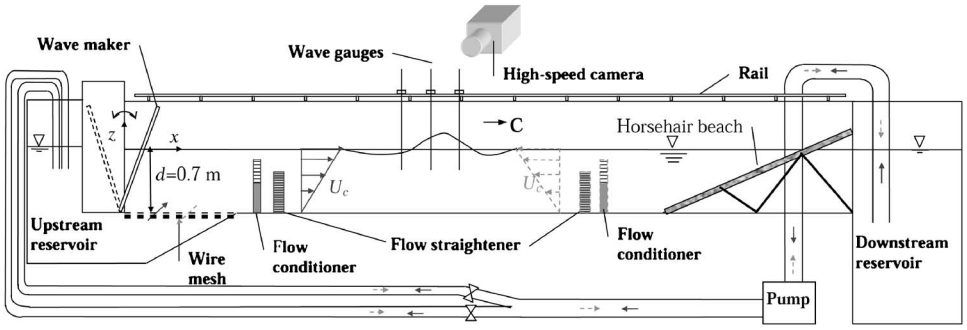

FIG. 1. Schematic of the wave-current flume and experimental setup.

flume, the wave-generation method of creating unsteady incipient breaking waves on vertically sheared currents, and the measurement technique is described in Sec. II. The results of measured wavelength, wave steepness, crest-trough asymmetry, and dimensionless amplitude of unsteady waves at incipient breaking are presented in Sec. III. Finally, the discussion and summary are given in Secs. IV and V, respectively.

II. EXPERIMENTAL APPROACH

A. Wave-current flume

The experiment was conducted in a wave-current flume at the University of Wisconsin-Madison (Fig. 1). The flume is 46 m long, 0.90 m wide, and filled with a water depth of $d=0.70$ m. A coordination system is defined in which the z-direction directs upwards from the still free surface, and the x-direction starts at the vertical position of the flap-type bottom-hinged wave maker. At the other end of the flume, a passive absorption wooden frame beach of a 1:10 slope, covered with 4-in.-thick porous horsehair mats, was installed. The beach was tested to absorb 95% of incident monochromatic waves.[26] Coexisting currents were achieved by a bidirectional, controllable centrifugal pump with a closed-loop pipeline. Following currents (in the same direction of wave propagation) were introduced by a sloping bed opening covered with a wire mesh in front of the wave maker. By reversing the pump, the water could go through the beach to create opposing currents.

B. Generation of sheared currents

A flow-shaping apparatus was devised and installed in the flume to generate controllable depth-varying current velocity profiles. The apparatus consists of two parts: a flow conditioner and a flow straightener (Fig. 1). The flow conditioner is made from two pieces of 1/4-in.-thick PVC plates held by a metal frame. The top PVC plate is perforated with 45% open area, while the bottom one was chosen either solid or perforated. Varying heights of the top and bottom plates were used to shape different current velocity profiles. A 2-in.-thick honeycomb block was placed 0.5 m downstream the flow conditioner to straighten the flow velocity. In the case of an opposing current, care was taken in placing the flow straightener and flow conditioner so that reflection waves were minimized at the time window of data collection. For both following and opposing currents, the free surface was maintained at least 0.1 m above the top of the perforated PVC plate and the honeycomb block.

A two-dimensional (2D)–three-dimensional (3D) acoustic Doppler velocimeter (10 MHz, SonTek, San Diego, CA) with an accuracy of 0.003 m/s was used to measure the current velocity at various water depths. Mean and turbulence velocities were calculated over 300 s (15 000 data points). Two typical mean velocity profiles in the x-direction, $U(z)$, are shown in Fig. 2(a). A following (opposing) current in the direction of wave propagation is represented by a positive (negative) velocity. Positive current shear $(U'=\partial U/\partial z>0)$ or negative current shear $(U'<0)$ is accordingly defined, based on the sign of the vertical gradient of a velocity profile near the free surface. To achieve the velocity profiles shown in Fig. 2(a), the flow straightener was placed at $x=3.3$ m and $x=14.0$ m for a following and an opposing current, respectively. In general, the streamwise velocity gradient $(\partial U/\partial x \leqslant 0.02)$ was approximately one order of magnitude less than the vertical shear $(U'=\partial U/\partial z \geqslant 0.15)$, indicating the overall dominance of the vertical shear. A quasisteady wave-current

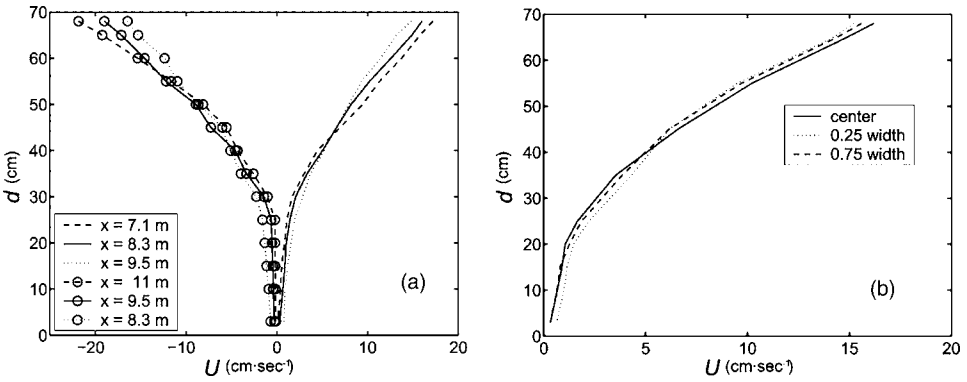

FIG. 2. (a) Mean velocity profiles at different longitudinal locations for a following current case 3 and an opposing current case 6. (b) Mean velocity profiles laterally across the flume at $x=8.3$ m for a following current (case 3).

flow therefore could be achieved where the characteristics of wave-current interaction are primarily dependent on the vertical current shear.[6,30] To avoid wave instability induced by a surface drift layer,[7,31] very strong vertical shear was not attempted here. In the absence of waves, the maximum surface disturbance of the fast current was less than 0.5 mm. The maximum lateral variation of the mean velocity profiles measured at 0.25-, 0.5-, and 0.75-widths of the flume was less than 5%, as shown in Fig. 2(b). In all the experimental cases, the maximum turbulence intensity was measured to be less than 10% using a time average of the 15 000 instantaneous velocity data points.

C. Unsteady focused waves on a sheared current

Based on linear wave theory, the free-surface displacement for a dispersive wave packet on a current at the wave maker position ($x=0$) is specified as

$$\eta(x=0,t)=\sum_{n=1}^{N} a_n \cos(k_n x-\omega_n t-\phi_n), \tag{1}$$

where a_n, k_n, ω_n and ϕ_n are the amplitude, wave number, radian frequency, and phase shift of the nth frequency component. $N=26$ components was chosen to evenly distribute ω_n within the frequency range of 0.8–1.8 Hz. On a coexisting sheared current, the wave number of each component k_n in the wave packet was calculated using the linear dispersion relation in the presence of a constant sheared current,[32,33] i.e.,

$$\omega_n = k_n U_s - \frac{U'}{2}\tanh k_n d + \left[\left(\frac{U'}{2}\right)^2 \tanh^2 k_n d + kg \tanh k_n d\right]^{1/2}, \tag{2}$$

where U_s is the surface velocity at the free surface, $U'=\partial U/\partial z$ is the current shear, g is the gravitational acceleration, and d is the water depth. The shear chosen here closely mimics the shear induced by wind forcing in the field, as seen in Fig. 2. A power-law wave spectrum was used to define the amplitude of each frequency component, i.e.,

$$a_n = G(k_n^0)^{-1.25}, \tag{3}$$

where G is a gain factorand k_n^0 is the wave number of the corresponding frequency component ω_n without current. In this study, an incipient breaking wave is defined as a nonbreaking wave for which even a slight increase in its steepness would cause breaking.[1,2] By increasing G, an incipient wave-breaking condition could be tuned with the aid of visual inspections.[1,2,25,26] Slightly above the incipient condition, a weak spilling breaker is initiated by the appearance of small ripples on the forward face of a steep wave crest.[34] These ripples have much shorter wavelengths compared to the input-generated waves so that they are easily discernible. In the experiment, the wave maker was controlled by a linear servo amplifier that was fed by voltage signals via a National Instrument (NI) AT-AO-6 data acquisition board with a 12-bit digitization (4096 counts) over a range of ±5 reference volts on a Pentium 133 master computer. The transfer function between wave amplitude and voltage can be obtained (approximately 5 cm/voltage), yielding an accuracy of 0.012 cm/count for an increment of G. In general, wave steepness between a weakest spilling breaker and an incipient breaking wave is found to be less that 0.0015, which is less than the typical variability of wave steepness for repeated experimental runs.

TABLE I. Experimental cases. The dashes indicate no applicable values of the focusing position.

Case	Wave frequency f (Hz)	Focusing position x_f (m)	Surface current velocity U_s (m s^{-1})	Surface current shear $U'_s=(\partial U/\partial z)_s$ (s^{-1})
1	0.8–1.8	8.3	0	0
2	0.8–1.8	8.3	0.13	0.15
3	0.8–1.8	9.28	0.167	0.4
4	0.8–1.8	6.9	0.225	0.8
5	0.8–1.8	9.7	−0.10	−0.15
6	0.8–1.8	9.7	−0.20	−0.5
7	1.8	-	0.0	0
8	1.8	-	0.167	0.4
9	1.8	-	−0.10	−0.15

To ensure all the frequency components in a wave packet were focused at a spatial location x_f and at a time instant t_f, each individual phase shift ϕ_n is initially set as

$$\phi_n = k_n x_f - \omega_n t_f + 2\pi m \quad (m=0,\pm 1,\pm 2,\ldots). \tag{4}$$

Equations (1)–(4) determine the designated time series of surface displacement generated by the wave maker, given a prescribed frequency range of a wave packet ϕ_n frequency and focusing time t_f and position x_f. As described previously, a transfer function of the wave maker $F(\omega_n, a_n)$ is required to transform $\eta(0,t)$ into the desired voltage input signal. The installation of the flow-shaping-and-straightener apparatus is expected to affect the transfer function. Therefore, an impulse-response method[25] within the frequency range of 0.2–2.0 Hz was used to determine any change of magnitude and phase in the transfer function for each experimental case of unsteady waves in Table I.

The concept of dispersive focusing method described above is essentially based on linear wave theory. Downshifting of the actual focusing position of incipient breaking has been documented,[1,26–29] which can be a concern of focusing incipient breaking at an undesired current shear location. To overcome this problem, a feedback-control focusing method is developed in this study. We first examine the phase $(\phi_n)_{\text{meas}}$ of each frequency component in the measured time series of surface displacement $\eta(x_f,t)$ from fast Fourier transform (FFT) analysis. Then an objective phase function Φ_n at $x=x_f$ and $t=t_f$ is set by

$$\Phi_n = (\phi_n)_{\text{meas}} - \omega_n t_f, \tag{5}$$

where Φ_n unwrapped between $\pm\pi$. If Φ_n is not zero, a correction is made to the initial phase shift ϕ_n so that a new input signal can be generated and re-sent to the wave maker. After two to four iterations, a very repeatable, unsteady wave

on a sheared current can be successfully generated at the prescribed spatial location and time instant.

The overall procedures of focusing a wave packet on a sheared current are summarized below: (i) a steady current of a desired vertical shear is created by the flow-shaping apparatus, and current velocity profiles over the depth and along the wave flume are measured; (ii) a range of wave frequencies ω_n is chosen and the corresponding wave numbers k_n are calculated using Eq. (2); (iii) the focusing position x_f and time t_f for a specific wave packet on the created current are selected based on current velocity profiles and the characteristic propagation speed of the wave packet; (iv) the amplitude a_n is determined using Eq. (3) and the initial phase shift ϕ_n for each frequency component is calculated using Eq. (4); (iv) the residue of he objective phase function Φ_n is used to update the initial or previous calculated phase, i.e., $(\phi_n)_{\text{updated}}=\phi_n-\Phi_n$; and (v) step (iv) is repeated until $\Phi_n=0$ to ensure the actual focusing of the incipient breaking condition at the prescribed position x_f and time t_f.

To examine the effects of vertically sheared currents on incipient unsteady breaking, a set of parameters (i.e., current velocity, direction, sign and magnitude of current shear, and focusing position) was varied in the present experiment, as shown in Table I. Overall, the repeatability of the incipient breaking waves on sheared currents was examined from at least three experimental realizations. The maximum variation in wave height was found to be less than 4%. The two-dimensional wave front was confirmed by measuring wave heights at 0.25-, 0.50-, and 0.75-widths of the flume at the focusing position x_f. The maximum cross-flume variation in wave height was less than 2%. The deviation of actual focusing time from the specified one was less than ±0.02 s. Finally, experiments for monochromatic wave trains by moving the wave maker in a sinusoidal function were conducted for the purpose of comparing with the unsteady wave cases. The amplitude was kept small to have overall wave steepness below 0.2. Very steep monochromatic waves up to breaking were not attempted to avoid the Benjamin-Feir stability problem.[7,30]

D. Measurement techniques

To measure wave profiles at incipient breaking, an automated digital imaging system was employed.[34] A high-speed camera (X-Stream VISION XS-3, Integrated Design Tools, Inc., Tallahassee, FL) fitted with a Nikon lens (28-mm $f/2.8$, Nikon Corp., Tokyo, Japan) was used to record images of fast moving and deforming surface waves at 100–200 frames/s. The image size is $1260\text{H}\times1024\text{V}$ with 8-bit depth. To acquire a complete wavelength (approximately 2 m), a back-lighting imaging technique was used. A wide imaging area was illuminated by a pair of halogen lights tilted upwards below the surface through the front sideglass of the flume. A highly reflective thin panel was adhered onto the back sidewall. The reflective panel served as an illuminating source for the water column, which eventually produced high contrast between air and water in digital images. After image acquisition, a robust and effective image-based measurement technique, active contour model, was applied to automatically delineate the surface wave profiles.[34] Measurements of wavelength was directly determined from two consecutive down-crossing points on each incipent breaking wave profile.

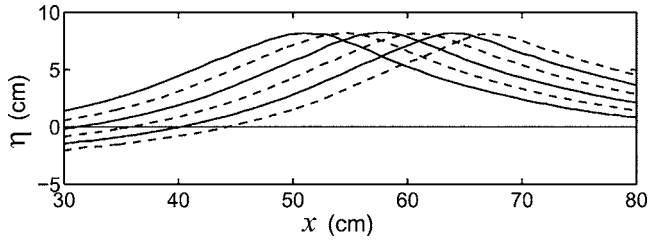

FIG. 3. Temporal and spatial evolutions of wave crest profiles for case 2. The solid and dashed lines are separated by a 0.025-s time interval.

Local wave phase speed was determined by the evolution of a temporal crest profile. For example, Fig. 3 shows a temporal evolution of a wave crest profile from the left to the right, separated by a time interval of 0.025 s. The third crest profile from the left corresponds to the focusing position. The wave crest moved at a fairly constant speed of 1.26 m/s for approximately 0.05 s. This speed should include the contribution from local wave phase speed (C) and surface current velocity (U_s). The local wave phase speed, therefore, was calculated by subtracting the surface current velocity in the absence of waves.

The time series of water surface displacement were measured with an array of capacitance-type wave gauges (Protecno S.R.L., Italy) mounted on movable carriages that travel on a rail on the top of the flume. During the measurement, all the movable carriages were locked at the specified positions. Prior to generating waves on a sheared current, the desired current was created first and elapsed at least for 1 h to achieve a steady-state water level, upon which the calibration of wave gauges was performed. The accuracy of the wave gauges was approximately ±0.5 mm, in comparison with video images of the same moving surface acquired by a planar laser-induced-fluorescence (PLIF) technique.[34] The time series of surface displacement provides an indirect method of calculating the wavelength. Conventional zero up-crossing methods[35] were used to determine the local wave period from which the corresponding wavelength was calculated using a dispersion relation.

III. RESULTS

A. Surface displacement

Success of the new feedback control (or iterative) frequency-focusing method in generating an unsteady incipient breaking wave on a sheared current at the specified position x_f and time instant t_f is illustrated. Figures 4(a) and 4(b) show the surface displacements and phases calculated from a single wave gauge fixed at the specified focusing position x_f for experimental case 2 ($x_f=8.3$ m, $t_f=19$ s). Since the actual focusing position without phase correction was downshifted from the prescribed location by approximately 0.4 m, a lower wave crest (dashed line) and the nonzero phases of the frequency components (open circles) were

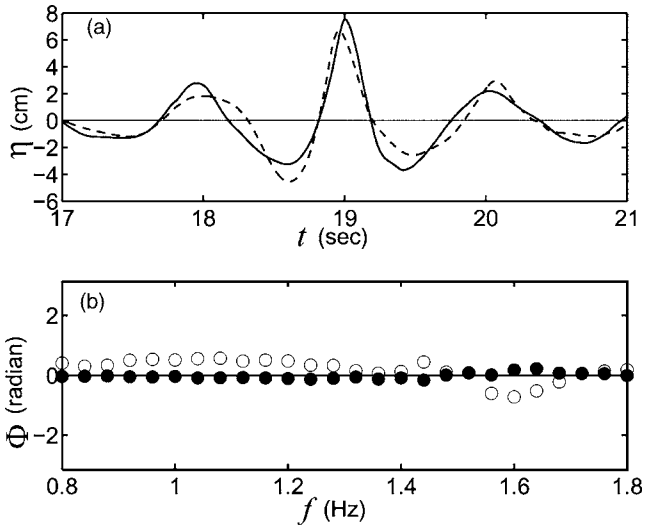

FIG. 4. An unsteady incipient breaking wave on a positively sheared current (case 2) generated by the iterative focusing method. (a) Surface displacement at the focusing position x_f before (---) and after (—) phase correction. (b) Phase function Φ of each frequency component before (○) and after (●) phase correction.

observed at x_f hrough the iterative focusing procedure, the phases (closed circles) were converged towards zero so that the growth of the incipient breaking wave crest on a positive current (solid line) was clearly observed. Similarly, for the incipient breaking wave on an opposing current in case 6, the success of spatial focusing at x_f=9.7 m and t_f=22 s was demonstrated the in the time series of the surface displacement in Fig. 5(a) and the phases of all frequency components in Fig. 5(b). The iterative focusing method effectively led to a zero phase for all wave components, yielding an incipient breaking wave crest at the prescribed position and time to meet the experimental condition.

B. Wavelength

The wavelengths of unsteady incipient breaking waves were measured from at least three repeated runs for each identical wave and current condition. Figures 6(a) and 6(b) show the recorded images for unsteady waves at incipient breaking on the positive and negative sheared currents in cases 4 and 5, respectively. For better visualization, the vertical scale was stretched by a factor of 4. Table II lists measured wavelengths for unsteady focusing waves and steady monochromatic waves in this study. In comparison with the measured wavelengths in the absence of a current (cases 1 and 7), a following current lengthens the wavelengths (cases 2 and 8) and an opposing current acts in the opposite way (cases 5 and 9), indicating the significant effects of Doppler shift on wavelength modulation. Surprisingly, on following currents with increasing surface velocity and positive shear (cases 2–4), the measured wavelengths show a slight-decrease trend, contrary to the previous reported results on steady waves on sheared currents.[36] Two possible explanations are provided here. First, in Eq. (2) the surface current velocity U_s and the current shear U' have opposite signs. As a result, lengthening of wavelengths on following currents ($U_s>0$) could be counteracted by positive current shear ($U'>0$). Second, it is recognized that nonlinearity can affect wavelength. As will be discussed in Sec. III C, positive shear reduces the limiting wave steepness. This reduction is proportional to the strength of the shear. Therefore, the descending limiting steepness from case 2 to case 4 could lead to the decrease of the corresponding wavelengths. Overall, Table II indicates the importance of not only the Doppler-shift effect, but also the vertical current profile (shear) and the nonlinearity in altering unsteady wave characteristics at incipient breaking.

A number of analytical dispersion relations for steady

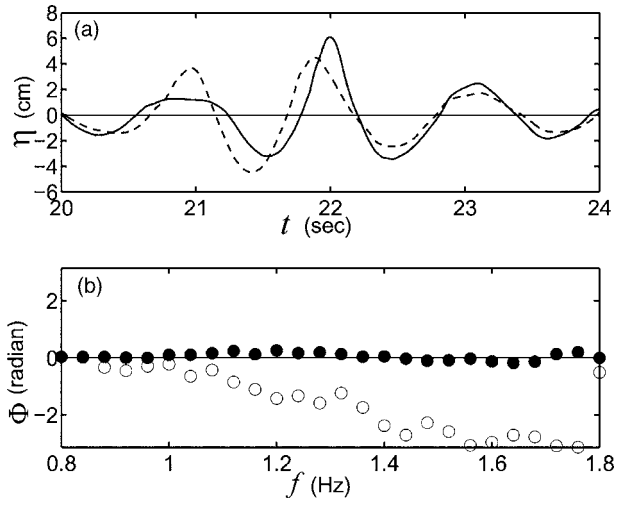

FIG. 5. Same as in Fig. 4 except for an unsteady incipient wave on a negatively sheared current (case 6).

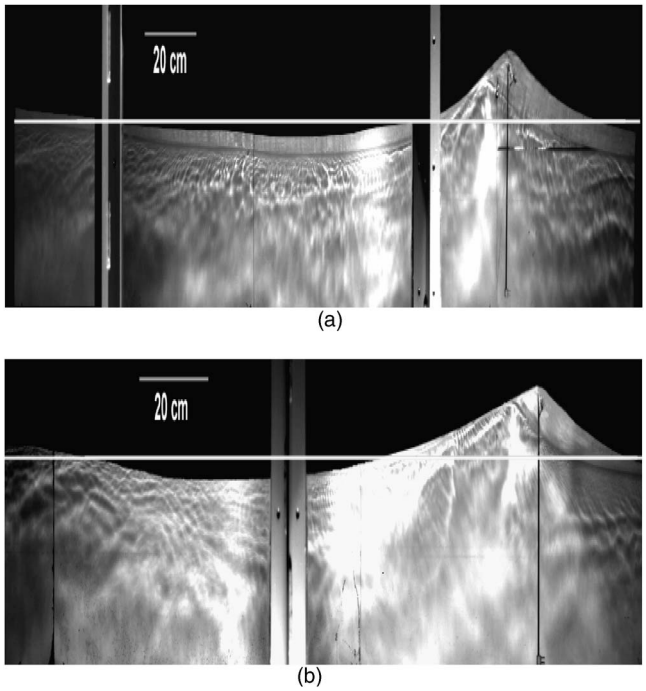

FIG. 6. Images for unsteady incipient waves on (a) a positive sheared current for case 4 and (b) a negative sheared current for case 5. A horizontal straight line marks the free surface in the absence of waves. A wave gauge was placed at the focusing position x_f.

TABLE II. Comparison of the wavelength using image measurements and dispersion relations.

Case	L (cm) Image measurement	Constant shear		Arbitrary shear
		L_l (cm) Linear dispersion relation (Ref. 32)	L_3 (cm) Third-order dispersion relation (Ref. 38)	L_a Second-order dispersion relation (Ref. 40)
1	171.79±1.8	149.13	153.48	149.13
2	202.39±4.5	163.17	167.22	163.08
3	201.62±2.5	164.08	168.34	164.53
4	198.70±3.3	165.46	169.03	167.18
5	165.78±2.1	126.80	131.31	126.72
6	162.20±5.8	112.11	113.20	114.54
7	49.22±0.6	48.18	49.46	48.18
8	64.41±0.8	63.47	65.38	63.45
9	38.37±0.5	36.80	38.60	36.82

monochromatic waves on currents of linear[32,33,37–39] and arbitrarily depth-varying profiles[32,40,41] have been previously derived. An excellent review on this topic is given by Thomas and Klopman.[7] To date, very limited experiments have been conducted to verify these dispersion relations in the regime of steady waves.[30,36] For unsteady waves, little is even known about their applicability. In this study, three dispersion relations for waves on sheared currents of linear or arbitrary profiles were used to estimate wavelength. For a constant shear profile, the linear dispersion relation is the exact solution of an inviscid Orr-Sommerfeld equation,[32] while the third-order dispersion relation is a perturbation solution of a Poisson equation.[38] For currents of arbitrary vertical shear, a second-order dispersion relation derived by Kirby and Chen[40] is used.

Table II also compiles a comparison between the measured and estimated wavelengths in this study. For steady monochromatic waves (cases 7–9), the wavelengths estimated by three dispersion relations are in close agreement with the measurements, consistent with previous experimental studies.[30,36] In particular, the third-order dispersion relation with a constant shear gives better estimated wavelengths with only 1.5% error, indicating the importance of wave nonlinearity. Moreover, these experimental results for steady monochromatic waves confirm the validity of the dispersion relations to infer wavelengths from the time series of the surface displacement, since these dispersion relations are essentially developed based on the assumption of steadiness and periodicity of wave forms. In contrast, for unsteady incipient breaking waves (cases 1–6) in Table II, these dispersion relations consistently underestimate the wavelengths up to 29.4% in comparison to the measurements from image analysis. Similar results using other dispersion relations[7,41] were also obtained, but not shown here for brevity. This underestimation of wavelength is believed to result from the rapid deformation of the wave profile and the considerable variation in wave speed during the evolution of a focused wave packet over one wave cycle.[27] In other words, a single wave period obtained from the time series of a focusing wave cycle cannot well characterize these unsteady wave features. Therefore, one should be cautious in applying the dispersion relations to estimate the wavelength of unsteady transient waves.

C. Steepness

The limiting wave steepness is defined as $\varepsilon=\pi H/L$, where H is the measured wave heights from the trough to the crest and L is the wavelength determined from two consecutive zero down-crossing points from image analysis. Figure 7 plots the wave steepness versus current shear for unsteady incipient breaking waves for cases 1–6 in this study. The vertical bars on wave steepness represent the variability among repeated experimental runs. The dependence of the limiting steepness on positive shear is apparent. For example, a positive shear in case 4, i.e., $\partial U/\partial z=0.8\ \mathrm{s}^{-1}$, reduced the limiting steepness by approximately 6%, in comparison to that in the absence of a current in case 1. This result is consistent with the reported value for a reduction of 5% in wave height due to a wind-driven positive shear.[42]

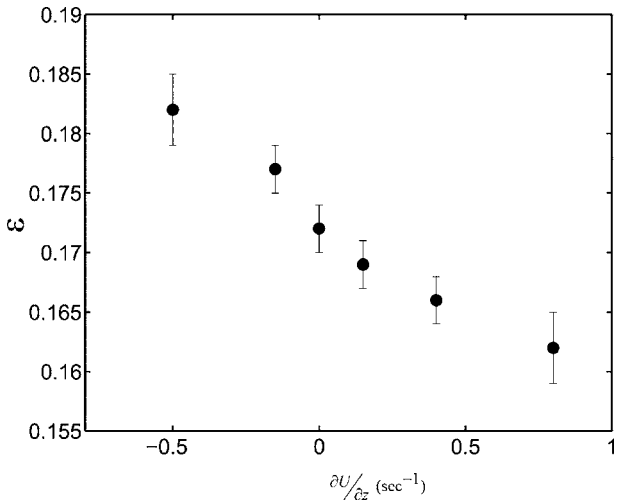

FIG. 7. Steepness of unsteady waves (ε) vs current shear ($\partial U/\partial z$) at incipient breaking. The vertical bars on wave steepness represent the variability among repeated experimental runs.

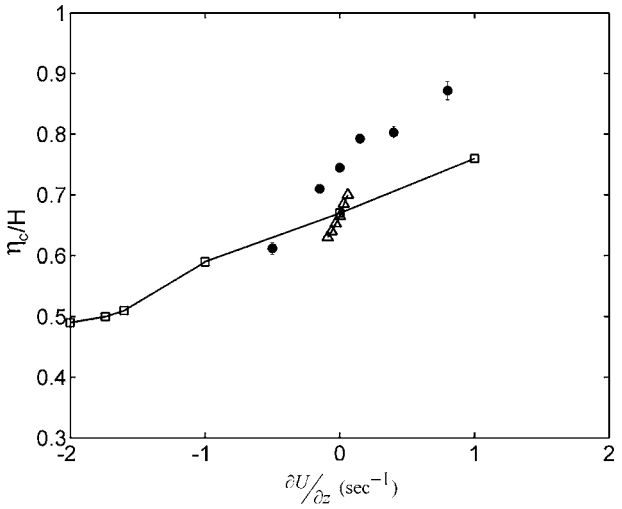

FIG. 8. Crest-trough asymmetry (η_c/H) vs current shear ($\partial U/\partial z$) at incipient breaking for unsteady waves from present experiment (filled circles), steady waves [solid line with triangles (Ref. 21)] and [solid line with squares (Ref. 17)]. The vertical bars indicate the variability of the asymmetry among repeated experimental runs. In some cases, the variability is less than the size of the data marker.

Overall, the presence of a positive current shear tends to reduce the limiting steepness. The magnitude of reduction in the wave steepness is proportional to the strength of the positive current shear.

In contrast, the presence of negative shear inhibits the onset of wave breaking, resulting in an increase of limiting steepness. In case 6, an opposing current with a negative shear, i.e., $\partial U/\partial z = -0.5\ \mathrm{s}^{-1}$, elevated the wave steepness nearly by 6%. Compared with a positive shear of the same magnitude, a negative shear appears to be more capable of modifying the steepness at incipient breaking, consistent with the trend obtained for steady extreme waves on sheared current.[17,18] However, the limiting steepness for unsteady waves is lower than that for steady waves. To the best of our knowledge, measurements on quantifying the role of a current shear on unsteady incipient breaking waves have not previously been reported.

D. Crest-trough asymmetry

The crest-trough asymmetry is defined as the ratio of the crest amplitude to the wave height, η_c/H, where η_c and H are measured directly from recorded images. This parameter has been widely used as a measure of feasibility of capsizing a marine vessel.[35] Figure 8 plots the crest-trough asymmetry versus the current shear of unsteady incipient breaking waves, shown as filled circles. The vertical bars indicate the variability of the asymmetry among repeated experimental runs. One can see that η_c/H shows a strong dependence on shear. The presence of a positive shear leads to an increased crest-trough asymmetry, while a negative shear results in decreased asymmetry. Interestingly, the trend of crest-trough asymmetry under the influence of a sheared current is opposite to that of the limiting wave steepness. An increased (decreased) crest-trough asymmetry is found for a positive sheared current in spite of a decreased (increased) limiting steepness. The modulated crest-trough asymmetry due to the presence of a current shear obtained in this study is consistent with that of monochromatic steady waves on sheared currents (shown as triangles and squares in Fig. 8).[17,21] However, the effect of a sheared current on crest-trough asymmetry is more pronounced for unsteady waves compared to those of limiting monochromatic steady waves. Under the same strength of a current shear, unsteady waves at incipient breaking generally experience higher crest-trough asymmetry than extreme steady waves, indicating the significant role of the vertical current profile (or vorticity) in modulating the crest-trough asymmetry of unsteady limiting wave profiles.

E. Dimensionless wave amplitude

In this section we further relate shear to the surface drift in order to correlate with the dimensionless amplitude of incipient breaking waves. For steady incipient waves, Banner and Phillips[16] theoretically predicted the maximum amplitude $\zeta_{\max}$ in the presence of a positive surface drift as

$$\zeta_{\max} = \frac{C^2}{2g}\left(1 - \frac{q}{C}\right)^2, \tag{6}$$

where q is the surface drift velocity at the point where the wave profile crosses the mean water level and C is the wave speed. Rearranging Eq. (6) under a deepwater assumption gives a dimensionless amplitude

$$Z_{\max} = \frac{2g\zeta_{\max}}{C^2} = \left(1 - \frac{q}{C}\right)^2. \tag{7}$$

Through detailed experiments and numerical simulations, Miller, Nennstiel, Duncan, Dimas, and Prostler[2] further modified the maximum amplitude of steady incipient breaking waves[17] as

$$Z_{\max} = \left(1 - \frac{q}{C}\right)^2 - 0.25. \tag{8}$$

For unsteady incipient breaking waves in the present experiment, $Z_{\max}$ was calculated using Eq. (7), where C is estimated as follows. The current velocity at the free surface U_s in the absence of the waves was used as the surface drift q. Local wave phase speed C was obtained by subtracting the measured wave crest speed at the focusing position us U_s. Readers should note that in Banner and Phillips[16] q was a "thin" vortical layer at the surface and the interior flow was assumed to be irrotational, which is not exactly the same as U_s under a "thick" current shear profile in this study [see Fig. 2(a)]. However, as indicated by Milinazzo and Saffman,[19] the product of the vorticity (or current shear) and the shear layer depth provides a good and useful measure of the surface drift velocity. In addition, the limiting wave crest speed (or limiting wave condition) has only a weak dependence on the shear layer depth and the main dependence is on the surface drift velocity. Therefore, the magnitude of U_s in this study may serve as an indicator of the approximate surface drift q. The purpose of using U_s, instead of shear, is to correlate with the dimensionless wave amplitude of wave breaking onset. Figure 9 shows the dependence of the dimensionless amplitude of incipient breaking waves on the normalized

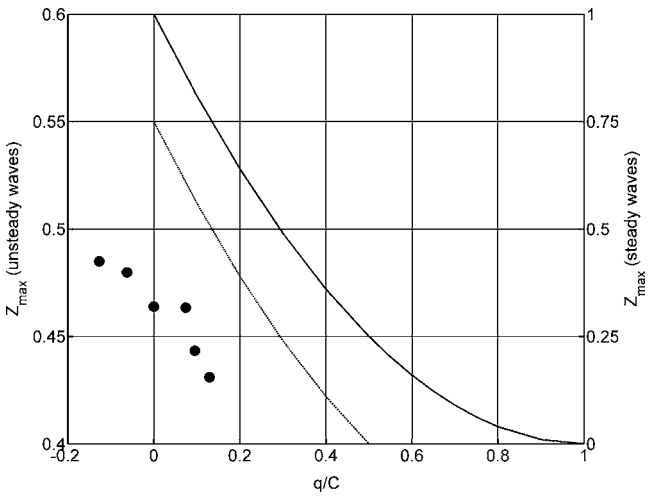

FIG. 9. Dimensionless wave amplitude vs normalized surface drift at incipient breaking for unsteady waves in the present experiment (filled circles) and steady waves by Banner and Phillips (Ref. 16), $Z_{max}=(1-q/C)^2$ (solid line), as well as Miller *et al.* (Ref. 2), $Z_{max}=(1-q/C)^2-0.25$ (dotted line).

surface drift, i.e., q/C. The dotted line and solid line represent the relationship for steady monochromatic waves at incipient breaking from previous studies.[2,16] Our measurements for unsteady waves exhibit a similar trend to those two curves for positive surface drifts in reducing the maximum dimensionless wave amplitude. In particular, the present experimental data extend to negative surface drifts (shear), favoring steeper incipient breaking waves. Moreover, it is found that the effects of surface drifts (surface shear) on steady and unsteady incipient breaking conditions are qualitatively the same, but quantitatively different (note that there are two different vertical scales in the figure). At the same surface drift, unsteady waves at incipient breaking have lower maximum dimensionless amplitude than steady waves. While this difference can be attributed to the effects of surface drift thickness on the modulation of the limiting wave condition, it is believed to be related to the dependence of the incipient breaking of unsteady waves on frequency bandwidth.[26] Further study is needed to reveal the role of surface shear (surface drift[16,19]) or bulk current shear in controlling the dimensionless amplitude of incipient breaking waves.

IV. DISCUSSION

To the best of our knowledge, this is the first experimental effort to confirm the previous computations of incipient breaking of unsteady waves on sheared[22,23] and advance our knowledge on this topic. Using a fully nonlinear numerical model, Banner and Tian[22] examined the onset of unsteady waves from self-modulating wave groups on a positive sheared current. They found that the limiting steepness of unsteady waves could be reduced up to 16% in the presence of positive shear $\partial U/z=0.2\ s^{-1}$. For subsequent improved self-modulating wave groups on a weaker positive background shear, Banner and Song[23] reported a consistent trend but a smaller reduction in the limiting steepness. In comparison, the wave steepness in the present experiment is even lower (i.e., 6% at the maximum positive shear $\partial U/\partial z=0.8\ s^{-1}$) than that of their computation results. This discrepancy might be caused by different wave group structures, i.e., frequency bandwidth, leading to different subsequent physical mechanisms to cause incipient breaking waves. In the present experiment, incipient breaking is generated by focusing wave packets of a relatively broad frequency bandwidth ($\Delta f/f_c=0.769$) in a very short time and distance. In the previous computational studies[22,23] the wave group is relatively narrow banded (e.g., $\Delta f/f_c=0.202$) and self-modulating. As a result, the onset of unsteady wave breaking could be mainly induced by the Benjamin-Feir instability. Further discussion on the dependence of wave steepness at incipient breaking on wave group structure (frequency bandwidth, spectral slope) can be found in Wu and Yao.[43] Their results suggest that the wave group structure is operative in determining the change on limiting steepness of unsteady waves.

The modified limiting unsteady wave profile due to a sheared current found in this study has important implications on the safety of navigation vessels and the design of marine structures. As shown in Fig. 7, the elevated wave steepness of the limiting wave can be caused by opposing currents with negative shear (e.g., inshore waves on ebb currents in tidal inlets[44]). It is known that wave steepness is a critical measure of navigation hazards at sea. A small vessel can ride over large and long waves provided they are not too steep, but large vessels could be significantly damaged or even capsized by a relatively small but steep wave.[45] As revealed in Fig. 8, the crest-trough asymmetry of limiting waves could be highly elevated due to positively sheared currents (e.g., wind driven currents[16]). The elevated crest-trough asymmetry can cause a high wave crest to inundate the structure far above the waterline crest, yielding tremendous pressure impact loadings of the so-called greenwater damage.[46,47] In addition, the enhanced crest-trough asymmetry of limiting waves creates severe bow damages of navigation ships due to a head-on collision of a moving vessel with a high wave crest. While the present experimental study has demonstrated the significant effects of a coexisting sheared current on the limiting wave profiles, the results are limited to a two-dimensional wave field and a collinear sheared current condition. In reality oceanic conditions are by far more complicated. Future studies on limiting three-dimensional waves under strong sheared current interactions, rapid varying bottom topographies, and extreme meteorological forcings in coastal and open seas are highly desired. Recently, some computational findings in this respect have been reported,[23,48] but further field and laboratory observations are still needed.

V. SUMMARY

Unsteady incipient breaking wave on both positively and negatively sheared currents is examined in this study. An iterative dispersive focusing method has been developed to generate incipient breaking waves by considering the effects of current shear and Doppler shift. Measurements of the surface displacement, the wavelength, and the wave phase speed

were made. Wavelengths measured directly from image analysis were compared with those inferred from the time series of the surface displacement using dispersion relations. Comparisons show that for steady monochromatic waves the dispersion relations taking into account a current shear work very well. In addition, a higher-order dispersion relation with constant shear gives better wavelength estimates with an error of less than 1.5%, indicating the importance of nonlinearity. However, a consistent underestimation of up to 29.4% is found when the dispersion relations are applied to unsteady incipient breaking waves, suggesting the significant modulation of wave characteristics during the evolution of a focused wave packet.

Wave steepness of unsteady incipient breaking is found to be altered by the sign and magnitude of a current shear. Positive current shear (such as that associated with a wind-driven current) reduces wave steepness, while a negative current shear (e.g., one found in an ebb current at a tidal inlet) acts in the opposite way. The magnitude of reduction/increase in wave steepness is proportional to the strength of a positive/negative shear. Negative shear appears to be more capable of changing the wave steepness in comparison to a positive shear of the same magnitude. Of interest, the trend of limiting wave steepness under the influence of a sheared current is in contrast to that of the crest-trough asymmetry. Increased crest-trough asymmetry, in spite of reduced limiting steepness, is attained for an unsteady incipient breaking wave on a positively sheared current rather than on a negatively sheared current.

The dimensionless amplitude for unsteady incipient breaking is correlated with normalized surface current drift. Increasing a positive surface drift leads to a reduced dimensionless wave amplitude. On the contrary, a trend of elevated dimensionless amplitude on increasing negative surface drifts is found. While the trend of dimensionless amplitude dependence on normalized surface current drift is consistent with that of steady monochromatic waves in previous studies,[2,16] the quantitative effects are different. Under the same surface drift, the unsteady waves would reach incipient breaking at a lower steepness than steady waves. With increasing surface drifts, the dimensionless amplitudes of unsteady waves descend at a slower rate than those of steady waves. These dissimilarities are believed to be related to the dependence of the incipient breaking of unsteady waves on frequency bandwidth.[26,43]

ACKNOWLEDGMENTS

This work is supported in part by the Office of Naval Research under Grants No. N00014-01-1-0268 and No. N00014-05-1-0091. The authors also acknowledge the instrument support grant from Wisconsin Alumni Research Foundation and College of Engineering at UW-Madison. The support from Dr. Mark Anderson and Professor Riccardo Bonazza at the Department of Engineering Physics at UW-Madison for providing the Spectral Physics Laser is acknowledged.

[1] R. J. Rapp and W. K. Melville, "Laboratory measurements of deep water breaking waves," Philos. Trans. R. Soc. London, Ser. A **331**, 735 (1990).
[2] M. Miller, T. Nennstiel, J. H. Duncan, A. A. Dimas, and S. Prostler, "Incipient breaking of steady waves in the presence of surface wakes," J. Fluid Mech. **383**, 285 (1999).
[3] M. A. Donelan, M. S. Longuet-Higgins, and J. S. Turner, "Periodicity in whitecaps," Nature (London) **239**, 449 (1972).
[4] L. H. Holthuijsen and T. H. C. Herbers, "Statistics of breaking waves observed as whitecaps in the open sea," J. Phys. Oceanogr. **16**, 290 (1986).
[5] A. V. Babanin, I. R. Young, and M. L. Banner, "Breaking probabilities for dominant surface waves on water of finite constant depth," J. Geophys. Res. **106**, 11659 (2001).
[6] D. H. Peregrine, "Interaction of water waves and currents," Adv. Appl. Mech. **16**, 9 (1976).
[7] G. F. Thomas and G. Klopman, in *Gravity Waves in Water of Finite Depth*, edited by J. N. Hunt (Computational Mechanics, Southampton, UK, 1997), pp. 215–319.
[8] J. Wu, "Wind-induce drift currents," J. Fluid Mech. **68**, 49 (1975).
[9] G. T. Csanady, "The free-surface turbulent shear-layer," J. Phys. Oceanogr. **4**, 402 (1984).
[10] L. M. Beal and H. L. Bryden, "The velocity and vorticity structure of the agulhas current at 32°S," J. Geophys. Res. **104**, 5151 (1999).
[11] I. G. Jonsson, in *The Sea: Ocean Engineering Science*, edited by B. Le Méhauté and D. M. Hanes (Wiley, New York, 1990), p. 65.
[12] A. T. Jessup, C. J. Zappa, and H. Yeh, "Defining and quantifying microscale wave breaking with infrared imagery," J. Geophys. Res., [Oceans] **102**, 23145 (1997).
[13] J. W. Peirson and M. L. Banner, "Aqueous surface layer flows induced by microscale breaking wind waves," J. Fluid Mech. **497**, 1 (2003).
[14] X. Zhang and S. Harrison, "A laboratory observation of the surface temperature and velocity distributions on a wavy and windy air-water surface," Phys. Fluids **16**, 1070 (2004).
[15] J. H. Duncan, "Spilling breakers," Annu. Rev. Fluid Mech. **21**, 519 (2001).
[16] M. L. Banner and O. M. Phillips, "On the incipient breaking of small scale waves," J. Fluid Mech. **65**, 647 (1974).
[17] J. A. Simmen and P. G. Saffman, "Steady deep-water waves on a linear shear current," Stud. Appl. Math. **73**, 35 (1985).
[18] A. F. Teles da Silva and D. H. Peregrine, "Steep, steady surface waves in water of finite depth with constant vorticity," J. Fluid Mech. **195**, 281 (1988).
[19] F. A. Milinazzo and P. G. Saffman, "Effect of surface shear layer on gravity and gravity-capillary waves of permanent form," J. Fluid Mech. **216**, 93 (1990).
[20] G. Breyiannis, V. Bontozoglou, D. Valougeorgis, and A. Goulas, "Large-amplitude interfacial waves on a linear shear flow in the presence of a current," J. Fluid Mech. **249**, 499 (1993).
[21] R. A. Dalrymple, A finite amplitude wave on a linear shear current," J. Geophys. Res. **79**, 4498 (1974).
[22] M. L. Banner and X. Tian, "On the determination of the onset of breaking for modulating surface gravity water waves," J. Fluid Mech. **367**, 107 (1998).
[23] M. L. Banner and J. B. Song, "On determining the onset and strength of breaking for deep water waves. Part II: Influence of wind forcing and surface shear," J. Phys. Oceanogr. **32**, 2559 (2002).
[24] M. Greenhow and T. Vinje, "A theoretical and experimental study of the capsize of Salter's Duck in extreme waves," J. Fluid Mech. **118**, 221 (1982).
[25] H. M. Nepf, C. H. Wu, and E. S. Chan, "A comparison of two- and three-dimensional wave breaking," J. Phys. Oceanogr. **28**, 1496 (1998).
[26] A. Yao and C. H. Wu, "Energy dissipation of unsteady wave breaking on currents," J. Phys. Oceanogr. **34**, 2280 (2004).
[27] C. H. Wu and H. M. Nepf, "Breaking wave criteria and energy losses for three-dimensional breaking waves," J. Geophys. Res. **107**, 3177 (2002).
[28] T. E. Baldock, C. Swan, and P. H. Taylor, "A laboratory study of nonlinear surface waves on water," Philos. Trans. R. Soc. London, Ser. A **452**, 649 (1996).
[29] T. B. Johannessen and C. Swan, "A laboratory study of the focusing of transient and directionally spread surface water waves," Proc. R. Soc. London, Ser. A **457**, 971 (2001).
[30] C. Swan, I. P. Cummins, and R. L. James, "An experimental study of two-dimensional surface waves propagating on depth-varying currents. Part 1. Regular waves," J. Fluid Mech. **428**, 273 (2001).
[31] E. A. Caponi, H. C. Yuen, F. A. Milinazzo, and P. G. Saffman, "Water-wave instability induced by a drift layer," J. Fluid Mech. **222**, 207 (1991).

[32]R. A. Skop, "Approximated dispersion relation for wave-current interactions," J. Waterw., Port, Coastal, Ocean Eng. **113**, 187 (1987).
[33]I. Kantardgi, "Effect of depth current profile on wave parameters," Coastal Eng. **26**, 195 (1995).
[34]A. Yao and C. H. Wu, "An automated image-based technique for tracking sequential surface wave profiles," Ocean Eng. **32**, 157 (2005).
[35]IAHR Working Group on Wave Generation and Analysis, "List of sea-state parameters," J. Waterw., Port, Coastal, Ocean Eng., **115**, 793 (1989).
[36]H. M. Nepf and S. G. Monismith, "Wave-dispersion on a sheared current," Appl. Ocean. Res. **16**, 313 (1994).
[37]S. Tsao, "Behavior of surface waves on a linearly varying current," Moskov. Fiz.-Tekh. Inst. Issled. Mekh. Prikl. Mat. **3**, 66 (1959).
[38]N. Kishida and R. Sobey, "Stokes theory for waves on linear shear current," J. Eng. Mech. **114**, 1317 (1988).
[39]R. E. Baddour and S. W. Song, "The rotational flow of finite amplitude periodic water waves on shear currents," Appl. Ocean. Res. **20**, 163 (1998).
[40]J. T. Kirby and T. M. Chen, "Surface waves on vertically sheared flows: Approximate dispersion relations," J. Geophys. Res. **94**, 1013 (1989).
[41]C. Swan and R. L. James, "A simple analytical model for surface water waves on a depth varying current," Appl. Ocean. Res. **22**, 331 (2000).
[42]A. D. Jenkins, in *Ocean Wave Measurement and Analysis, Proceedings of WAVES 2001*, San Francisco, 2001, edited by B. L. Edge and J. M. Hemsley, pp. 494–500.
[43]C. H. Wu and A. Yao, "Laboratory measurements of limiting freak waves on currents," J. Geophys. Res. **109**, C12002 (2004).
[44]F. I. Gonzales, E. D. Cokelet, J. F. R. Gower, and M. R. Mulhern, in *The Ocean Surface*, edited by Y. Toba and H. Mitsuyasu (D. Reidel, New York, 1985), pp. 303.
[45]E. A. Dahle and D. Myrhau, "Risk analysis applied to capsize of fishing vessels," Marine Tech. Sname News **32**, 245 (1995).
[46]R. G. Bea, T. Xu, J. Stear, and R. Ramos, "Wave forces on decks of offshore platforms," J. Waterw., Port, Coastal, Ocean Eng. **125**, 136 (1999).
[47]C. Guedes Soares, Z. Cherneva, and E. M. Antão, "Steepness and asymmetry of the largest waves in storm sea states," Ocean Eng. **31**, 1147 (2004).
[48]J. B. Song and M. L. Banner, "Influence of mean water depth and a subsurface sandbar on the onset and strength of wave breaking," J. Phys. Oceanogr. **34**, 950 (2004).